Space Science Reviews (2023) 219:47
https://doi.org/10.1007/s11214-023-00993-9

Cross-Validation of the Ionospheric Vertical Drift Measurements Based on ICON/IVM, Swarm, and the Ground-Based Radar at the Jicamarca Radio Observatory

Yen-Jung J. Wu[1] · Stephen Mende[1] · Brian J. Harding[1] · Patrick Alken[2,3] · Astrid Maute[2,3] · Thomas J. Immel[1]

Received: 2 January 2023 / Accepted: 10 August 2023

Abstract
The Ion Velocity Meter (IVM) on NASA's Ionospheric Connection Explorer (ICON) reports the in-situ ion density, ion temperature and 3-component ion drift velocity, retrieved from measurements by a retarding potential analyzer and an ion drift meter. ICON was launched during a deep solar minimum in late 2019, followed by a solar quiet (F10.7 < 80) period until September 2020. In order to quantify the uncertainties in the IVM's drift velocity in a low plasma density environment, we compared IVM's vertical drift velocity with eastward electric field (EEF) obtained from Swarm's equatorial electrojet current measurements, the vertical drift from ground-based incoherent scatter radar (ISR) at Jicamarca Radio Observatory (JRO) and from Jicamarca Unattended Long-term studies of Ionosphere and Atmosphere (JULIA) coherent mode. The main results of this study show that (1) the vertical drift derived from Swarm's EEF and ISR are in good agreement with the zonal electric field derived from JULIA's vertical drift regardless of the F10.7 value. (2) The zonal electric field derived from IVM's meridional drift is in good agreement with Swarm's EEF in 2021, whereas the distribution is highly scattered in the deepest solar minimum in 2020. (3) An ad hoc IVM correction based on the 24-hour running mean of meridional drift can bring the IVM data into better agreement with Swarm and JULIA. An additional quality control based on O^+ fractional composition may be needed for some studies using IVM's vertical drift. By using the same methodology presented in this work, future missions could calibrate their drift measurements to facilitate meaningful integration with ICON/IVM observations through the comparision with ground-based measurements.

Keywords Equatorial ionosphere · Vertical ion drift · Ionospheric Connection Explorer · Ion drift meter · Jicamarca Radio Observatory

The Ionospheric Connection Explorer (ICON) Mission: First Results
Edited by David E. Siskind and Ruth S. Lieberman

✉ Y.-J.J. Wu
yjwu@ssl.berkeley.edu

1 Space Sciences Laboratory, University of California, Berkeley, CA, USA

2 University of Colorado, Boulder, CO, USA

3 National Centers for Environmental Information, Boulder, CO, USA

Published online: 07 September 2023

1 Introduction

Ionospheric Connection Explorer (ICON) launched into a Low-Earth Orbit at ~600 km with 27° orbit inclination in 2019 to study the interaction between the lower atmosphere and the highly variable ionosphere (Immel et al. 2018). ICON is equipped with instruments measuring both ionospheric and neutral atmospheric components. Neutral wind vectors and temperatures are retrieved from the Michelson Interferometer for Global High-resolution Thermospheric Imaging (MIGHTI) (Harding et al. 2017; Harlander et al. 2017; Englert et al. 2017; Stevens et al. 2018), and O/N_2 density ratio are derived from the airglow emission observed by the FUV imager (Mende et al. 2017) in the daytime. For the ionospheric quantities, EUV (Stephan et al. 2018) and FUV imagers provide O^+ density profile in the daytime and nighttime, respectively. In addition to the aforementioned remote-sensing instruments, the Ion Velocity Meter (IVM) measures in-situ ion density, ion temperature and 3-components of the ion drift velocity, at the orbit altitude ~600 km (Heelis et al. 2017) in the topside ionosphere above the F-layer density peak altitude. ICON provides unique observations to understand ionospheric electrodynamics when the spacecraft is near the magnetic equator, during which the MIGHTI wind measurements in the E-region are magnetically connected to the ICON/IVM's measurements. This alignment provides the necessary conditions to investigate the influence of the wind dynamo effect on the ionosphere on the same magnetic field line (Immel et al. 2021).

ICON/IVM shares the same design with the IVM on the Communications and Navigation Outage Forecasting System (C/NOFS) satellite and COSMIC-2 (Schreiner et al. 2020). Heelis et al. (2017) described the detailed design, pre-flight instrument calibration, and uncertainty analysis of ICON/IVM. A retarding potential analyzer (RPA) and an ion drift meter (IDM) are the two major sensors on IVM to determine the energy of the incoming ions and the arrival angle of the ion flows, respectively. The ion density, major ion fractions and temperature are retrieved from fitting the curve of the integrated current measured by RPA as a function of step-in voltage. The 3-dimensional ion drifts require simultaneous measurements from both RPA and IDM. The cross-track components of the ion drift are derived from the combination of the ram ion drift measured by RPA and the angle of arrival resolved by IDM. Since O^+ is the heavier and typically more dominant species than H^+ around 600 km in the ionosphere, the uncertainty of the ion drift measurement is influenced by the total ion density and the O^+ fraction. The largest uncertainties occur when both the total ion density and the O^+ fraction are low, producing higher errors in both RPA and IDM, and resulting in low sensitivity in the ram drift from RPA. To achieve the scientific goal of the ICON mission, ICON/IVM is designed to measure the meridional drift at low latitudes, with a dynamic range $\pm$ 750 m/s and accuracy of 7.5 m/s. The pre-flight uncertainty analysis (Heelis et al. 2017) demonstrated that the root-mean-square error (RMSE) of the ram ion drift velocity should be less than 10 m/s when O^+ fraction is greater than 0.2 and O^+ density is larger than $10^4/cm^3$. Immel et al. (2021) used ICON data to show the first direct evidence connecting variability in the equatorial vertical drift with lower thermospheric winds. Due to IVM offsets occurring during the very low F10.7 conditions in early 2020, they found it necessary to preprocess the IVM data to force the 24-hour-mean meridional drift to be zero.

Cross-platform validations are crucial to independently evaluate the data quality of the space-borne plasma measurements when the observatory is in orbit. The outcome not only provides the relative measurement uncertainties of the new data set with respect to the existing dataset, but also often reveals the temporal or spatial variation of the uncertainties due to different geophysical conditions. Chou et al. (2021) compared two independent measurements on COSMIC-2, IVM ion density and Tri-GNSS Radio-Occultation System (TGRS)

orbit electron density and found that the mean difference is less than $|0.03 \times 10^4|/\text{cm}^3$. The authors also pointed out that the mean difference is larger in the nighttime compared to daytime due to the error from the low background density in the nighttime. Choi et al. (2023) reported the comparison of the ion density measured by COSMIC-2/IVM and ICON/IVM using measurements $\sim$ 50 km apart in altitude. The authors stated that the climatology of the diurnal variation and the interhemispheric asymmetry of the ion density distributions between the two measurements are similar, but the nighttime (daytime) ion density observed by ICON/IVM is slightly greater (lower) than COSMIC-2. Stoneback et al. (2012) reported the comparison of the vertical drift between the measurements from the Jicamarca incoherent scatter radar and IVM on C/NOFS. The results show an excellent correspondence between the two measurements as a function of local time (LT) in a total of 8 days of data, supporting the methodology used to extract ion drift from C/NOFS. Through the relation of the electric field and the cross product of the drift velocity and magnetic field ($E = v \times B$), Alken et al. (2015) validated the daytime equatorial electric field (EEF) derived from magnetic field signatures measured by European Space Agency (ESA)'s Swarm satellites (Friis-Christensen et al. 2006) with the vertical ion drift of the 150 km echo measured by Jicamarca Unattended Long-term studies of Ionosphere and Atmosphere (JULIA) coherent mode at the Jicamarca Radio Observatory (JRO) (Kudeki and Fawcett 1993). The correlation between Swarm's EEF and JULIA is high ($r = 0.78$), and the best line fit shows the slope close to 1.

In this study, we focus on the cross-comparison of the vertical drift (zonal electric field) near the magnetic equator measured by ICON/IVM, the EEF obtained by Swarm, and the vertical drift from the VHF incoherent scatter radars (ISR) and 150 km echo from the JULIA mode at JRO. The main target of this validation work is to quantify the error in the ICON/IVM vertical drift, with a secondary goal of evaluating the efficacy of quality-control and pre-processing algorithms. The introduction to the data and method of finding conjunctions between two measurements is given in Sect. 2. The results of the correlation analysis among all these measurements are discussed in Sect. 3. In Sect. 4, we revisit the assumption of zero mean vertical drift taken in Immel et al. (2021). The discussion and the main result are summarized in Sect. 5 and Sect. 6, respectively.

2 Data and Data Selection

The ICON/IVM data product represents the drift vector in magnetic coordinates, with the variable ICON_L27_Ion_Velocity_Meridional perpendicular to the magnetic field (B) and pointing in a poleward direction, which is the component corresponds to the vertical drift near the magnetic equator. Our analysis is based on version 06 of the ICON/IVM dataset, and we have specifically utilized data with no flagged quality issues in both the drift meter flag (ICON_L27_DM_Flag = 0) and the RPA flag (ICON_L27_RPA_Flag = 0). It is worth noting that future versions of the dataset may address identified errors and implement improvements to quality control.

The VHF ISR located at JRO (geographic coordinates 11.8S, 77.2W; geomagnetic dipole latitude 0.8S) have been instrumental in equatorial ionospheric studies for several decades. These radars provide valuable and unique observations of various ionospheric parameters, including electron density, thermal structure, and ion compositions. At JRO, two types of vertical drift observations are provided at different altitude ranges: drift profiles in the F-region ranging from 200 km to 600 km, and daytime vertical drift in the E-region. The F-region drift profiles are obtained using the high-power incoherent mode, which involves measuring the line-of-sight ion velocities with uncertainties of 0.5-1.0 m/s (Kudeki et al.

1999). On the other hand, the E-region vertical drift is derived from 150-km echoes using the low-power coherent mode, also known as the JULIA mode (Kudeki and Fawcett 1993; Chau and Kudeki 2006). Chau and Woodman (2004) have confirmed a strong agreement between the vertical drift obtained from the 150-km echoes and the F-region drift, supporting the use of JULIA data at 150 km to corroborate ICON/IVM drift measurements at approximately 600 km. Conjunctions between the satellite missions (ICON and Swarm) and JULIA are considered successful when they occur within 20 degrees longitude and 5 degrees latitude of JRO, with a time difference no larger than 10 minutes. In the years 2020 and 2021 between LT 11 to 17, a total of 200 ICON/IVM-JULIA conjunctions have been identified and utilized to investigate the uncertainty of ICON/IVM drift measurement in this study. Similarly, for the ICON/IVM-ISR conjunctions, a comparable RMSE to that of the ground-based measurement was achieved by selecting IVM data within 20 degrees longitude and 5 degrees latitude of the JRO site, with a time difference not exceeding 10 minutes. A total of 89 ICON/IVM-ISR conjunctions were identified for analysis.

The equatorial electrojet (EEJ) manifests as a strong zonal (east-west) current predominantly observed in low-latitude regions during the daytime. Its intensity is influenced by the interplay between the vertical polarization electric field and the nearly horizontal magnetic field at the equator. The Swarm satellite constellation, operating in a polar orbit, facilitates the acquisition of scalar magnetic field measurements that encompass comprehensive latitudinal coverage. The Sq contribution is isolated by employing spherical harmonic expansion techniques thereby enabling the retrieval of EEJ and the EEF in the E-region (Alken and Maus 2010). In a comparative investigation, Alken and Maus (2007) explored the relationship between the EEJ current and the corresponding eastward electric field inferred from vertical drift, considering both cases with and without accounting for conductivity. The findings demonstrated a notable enhancement in correlation, increasing from 0.83 to 0.91 when the estimated conductivity was incorporated, namely multiplying electric field by the conductivity. In the Swarm data, the relative error (RelErr) of EEF is quantified as the difference between the satellite-derived and modeled current profiles divided by the satellite-derived current (Alken et al. 2015). For the purposes of this study, we consider only the Swarm EEF data with a RelErr value of less than 2 in the performed comparisons. This criterion ensures the inclusion of data points with acceptable levels of measurement and retrieval error.

The cross comparison of the measured vertical drift (zonal electric field) measured by ICON and estimated by Swarm magnetic field measurements necessitates the occurrence of a conjunction between the two satellites. A successful ICON-Swarm conjunction is achieved when both satellites closely intersect in space and time, during daytime (LT 11-17) in proximity to the magnetic equator. Figure 1 provides an illustration of such a conjunction occurring at the magnetic equator. The diagram showcases multiple dipole-like field lines, with the highest apex corresponding to the altitude of the ICON orbit ($\sim$600 km). ICON, following a low inclination orbit, predominantly moves eastward (out of the paper, towards the viewer), while Swarm travels in a north-south direction (right-left, parallel to the plane of the paper). The region where EEJ flows aligns with areas of heightened conductivity within the Cowling region, depicted in yellow. Additionally, the diagram highlights the relatively high conductivity E region through a thick dashed line, spanning altitudes ranging from 100 to 130 km. Throughout the 11 to 17 solar LT on the dayside, we have identified a total of 107 ICON-Swarm conjunctions during the years 2020 and 2021. To meet the criteria for conjugacy, the two satellites were required to be horizontally separated by no more than 2000 km and within a 20-minute time window of each other at the point of equator crossing.

To ensure a valid intercomparison of electric fields and related drift measurements taken at different altitudes, it is important to understand how electric fields vary with altitude at the

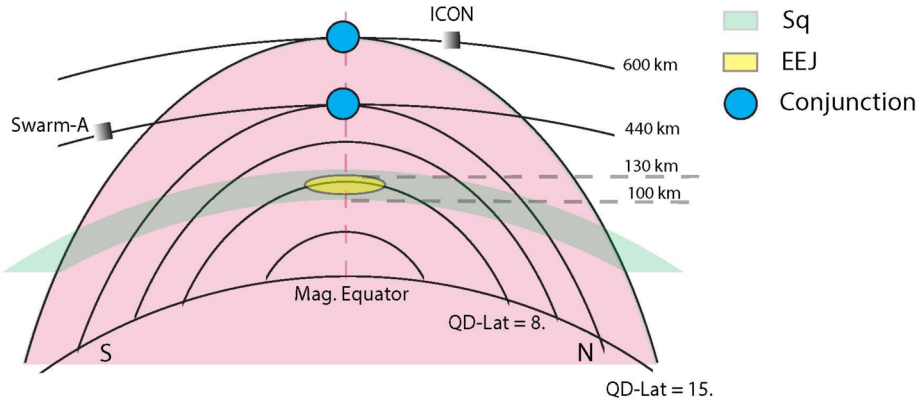

Fig. 1 Schematic illustration of a view looking westward parallel to the magnetic equator. See the text for the description. Quasi-dipole (QD) magnetic latitude is applied

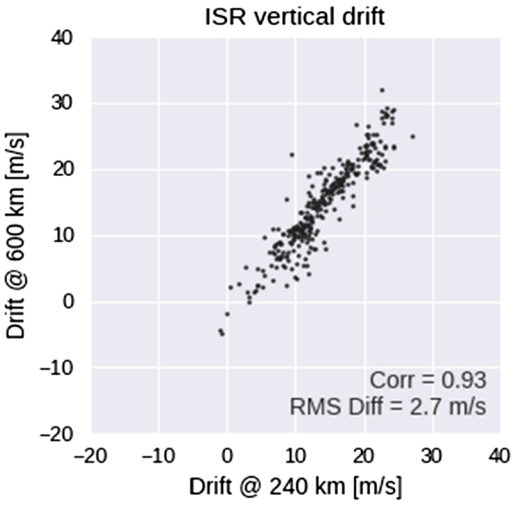

Fig. 2 The vertical drift at 240 km against the vertical drift at 600 km, measured by the JRO ISR for all available data between 10 and 17 LT from Dec 2019 – Sep 2021

equator. Previous studies have already demonstrated the agreement between average vertical drifts at 150 km altitude and model predictions of F-region drifts (Chau and Woodman 2004; Rodrigues et al. 2015). Additionally, Shidler and Rodrigues (2019) have shown that the average altitudinal gradient of the vertical drift from 200 km to 600 km at the magnetic equator is small during the daytime, supporting the assumption that vertical drift measurements at different altitudes are comparable and can be mutually validated. To further substantiate this assumption, we present Fig. 2, which depicts the comparison of vertical drift measurements from the ISR at 240 km with those at 600 km. The analysis covers the period between 10 to 17 LT from December 2019 to September 2021 during geomagnetic quiescence. The correlation coefficient is calculated to be 0.93, and the RMSE is 2.7 m/s. This high correlation indicates that over 86% of the variability in the topside (600 km) ionosphere drift can be explained by the drift at the bottomside (240 km) during the daytime. Based on these findings, it is reasonable to compare the vertical drift measured by ICON/IVM at 600 km, the vertical drift associated with the zonal EEF at 110 km, and the vertical drift measured at 150 km.

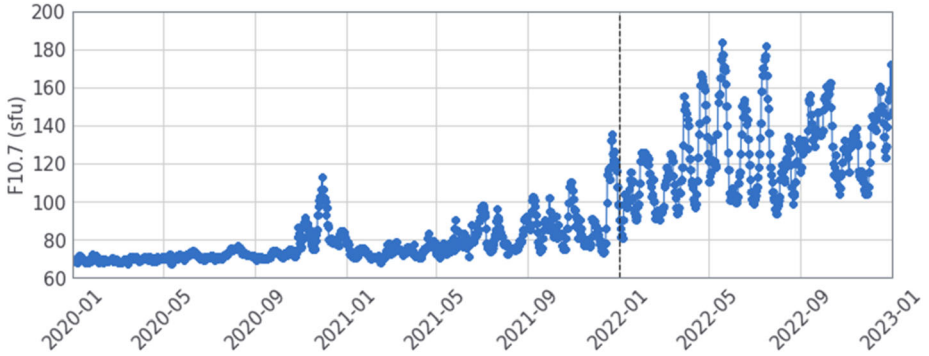

Fig. 3 F10.7 solar index from 2020 to the end of 2022

Moreover, given the RMSE of 2.7 m/s shown in Fig. 2, we consider the altitude gradient of the vertical drift to be a negligible issue for our study.

3 Results

ICON was launched at a deep solar minimum in 2019/2020 during which the F10.7 index was approximately 70 sfu for most of the time before October 2020, followed by a dramatic pulse-like variation of F10.7 reaching 113 sfu in November 2020 on top of a gradual increase in 2021 that surpassed 80 sfu in April 2021 (Fig. 3). The high correlation between JULIA vertical drift and Swarm EEF reported by Alken et al. (2015) was under a solar maximum condition from November 2013 to October 2014. Therefore, we revisit the work with the data in the most recent solar minimum to see whether the significant difference in solar radiation has an impact on the Swarm EEF-JULIA comparison. Figure 4 shows the distribution of the EEF from Swarm-A against JULIA vertical drift. The resulting correlation coefficient is 0.89 and the slope of orthogonal distance regression is 1.18, while Alken et al. (2015) reported a correlation of 0.8 and a slope of 1.14. This result indicates that the high correlation between Swarm-A and JULIA vertical drift reported by Alken et al. (2015) also holds at solar minimum. The magnetometer measurement not requiring an abundant ambient ion density may grant the stable Swarm-JULIA relation, despite electric field and magnetic perturbations reportedly being affected by the geomagnetic conditions.

The JULIA coherent radar serves as a valuable ground truth reference to validate both ICON and Swarm measurements at a specific location, while the conjunctions between ICON and Swarm provide cross-validation over a broader spatial range. Figure 5 illustrates the comparison between IVM's vertical drift and the JULIA vertical drift for radar conjunctions in 2020 and 2021. In Fig. 5a, during the deep solar minimum of 2020 (with an annual median F10.7 of approximately 75 sfu), the distribution of data points exhibits significant scattering. However, as shown in Fig. 5b, the correlation between the two datasets improves in 2021, corresponding to an increase in F10.7 values (with an annual median F10.7 of around 87 sfu). The correlation coefficient increases from 0.51 in 2020 to 0.64 in 2021, while the slope of the relationship changes from 0.18 to 0.38. Figure 5b also reveals that the data points for 2021 with a low O^+ fraction (represented by blue dots) tends to deviate from the dashed unity line. Note that the line fitting in this study is performed by orthogonal distance regression to reduce the influence of the outliers in the distribution. This observation

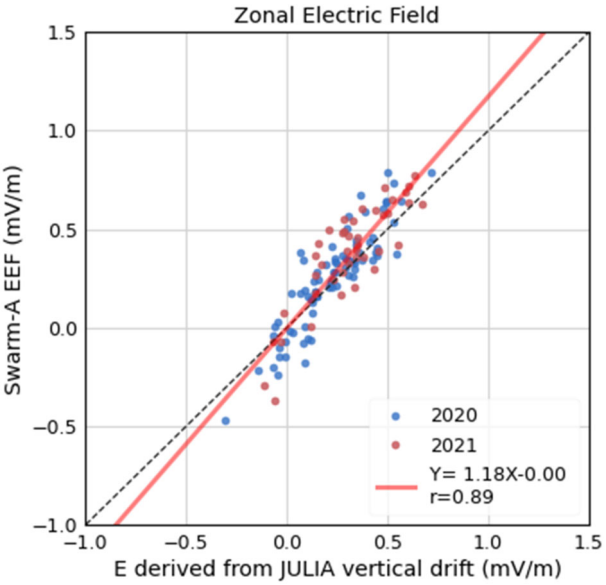

Fig. 4 Scatter plot comparing the zonal electric field derived from JULIA vertical drift measurements and the equatorial electric field from Swarm-A, between 11 and 17 LT spanning from January 2020 to May 2021. The black dashed line represents a slope of 1, indicating a one-to-one relation between the two parameters. The red solid line represents the linear regression based on all data from 2020 and 2021

suggests a potential relationship between the error of the IVM drift measurement and the ambient O^+ fraction and density. The finding is consistent with expectations, as the instrument exhibits greater sensitivity in an O^+-rich plasma environment compared to an H^+-rich plasma environment.

To establish general criteria based on O^+ density and O^+ fraction, Fig. 6a illustrates the RMSE between ICON/IVM and JULIA vertical drift as a function of O^+ fraction and O^+ density, which are used as the lower limits for data selection. The corresponding sample count under each condition is presented in Fig. 6b. It is worth noting that when the sample size is large (i.e., sample size ≥ 31 or degree of freedom ≥ 30), the Student t-density function closely approximates the normal distribution, making the application of the Central Limit Theorem statistically meaningful for using sample averages to represent the expected value of an unknown population (Wong et al. 2009; Freedman et al. 2007). Based on the analysis of all conjunctions in 2020 and 2021, Fig. 6a demonstrates a clear transition in the RMSE, shifting from values greater than 15 m/s to less than 10 m/s when an O^+ fraction greater than 0.8 is applied, regardless of the O^+ density value. This condition yields a total sample count of approximately 30. On the other hand, if an O^+ density of $2 \times 10^5/\text{cm}^3$ is used as the lower bound, the same level of RMSE less than 10 m/s can be achieved, although with a reduced sample count of fewer than 20. Consequently, the utilization of an O^+ fraction greater than 0.8 as an advanced data quality control criterion is preferable over relying solely on O^+ density.

Returning to scatter plots depicted in Fig. 5, Fig. 5c presents a scatter plot including all ICON/IVM-JULIA conjunctions in 2020 and 2021, showing a correlation coefficient of 0.53. However, the RMSE is relatively high, reaching approximately 19.90 m/s. By imposing a constraint of O^+ fraction > 0.8 for testing purposes (Fig. 5d), the correlation for the combined dataset from 2020 and 2021 improves to 0.71, accompanied by an increased slope of 0.56. As a result, the RMSE is significantly reduced to 6.41 m/s with a sample count of 34. Despite the improvement, the slope of 0.56 indicates that the IVM measurement is approximately twice as large as the vertical drift reported by JULIA. While the constraints

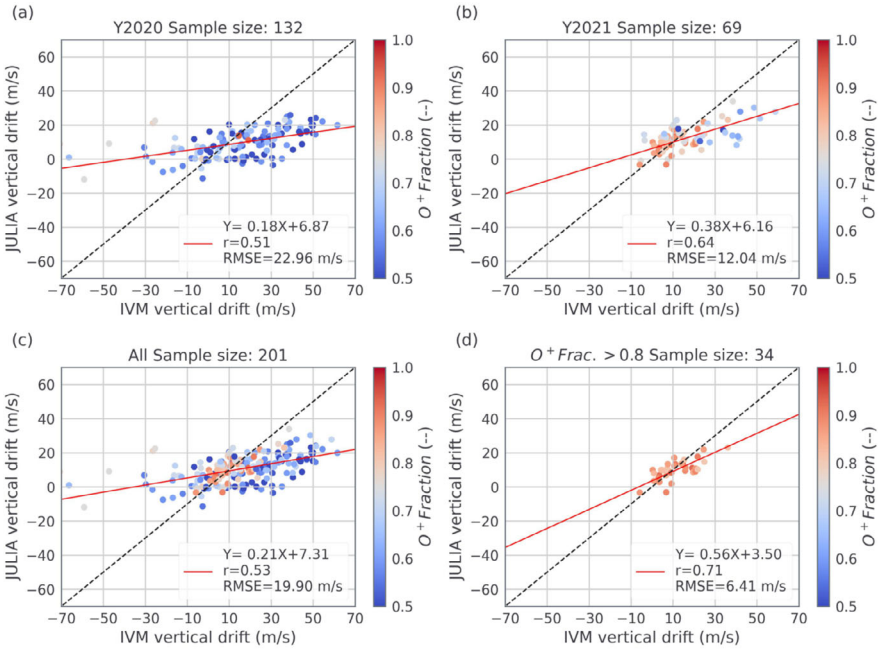

Fig. 5 Scatter plots comparing vertical drift measurements between JULIA and ICON/IVM between 11 and 17 LT for the years 2020 (a) and 2021 (b). Panel (c) displays the total conjunctions for both years, while panel (d) presents the conjunctions limited to an criterion of O^+ fraction >0.8. Successful ICON/IVM-JULIA conjunction is when IVM is within 20 degrees longitude and 5 degrees latitude from JULIA, with measured time difference less than 10 minutes. The black dashed line represents a slope of 1, indicating a one-to-one relation between the parameters. The red solid line represents the linear regression function. The linear function, correlation coefficient, and root-mean-square difference are indicated in the lower-right corner of the plots

used in this study, specifically an O^+ fraction > 0.8, exceed the recommended levels proposed in Heelis et al. (2017) based on pre-flight calibration, the observed slope of 0.56 suggests two potential scenarios. First, there may be additional unknown factors influencing the absolute magnitude of the measured drift by IVM, beyond the influence of O^+ fraction alone. Second, the bias could potentially lie on the side of the JULIA measurements. To further investigate and validate these scenarios, incorporating a third measurement source would provide additional insights and help elucidate the contributing factors to the observed discrepancies.

Moving on to the ICON/IVM-Swarm conjunctions, to ensure consistency in drift measurements, we calculate the vertical ion drift by dividing EEF by the magnetic field magnitude obtained from the International Geomagnetic Reference Field (IGRF) at 110 km altitude. The ICON/IVM-Swarm comparison is presented in Fig. 7a for 2020 and Fig. 7b for 2021. The results reveal a similar level of agreement as observed in the ICON-JULIA comparison. In 2021, the correlation coefficient improves to 0.77 compared to 2020, and the RMSE decreases from 13.55 m/s to 8.26 m/s. Applying the same criteria used for the ICON-JULIA conjunctions, Fig. 7c showcases the data combining both 2020 and 2021, while Fig. 7d presents the scatter plot with the additional constraint of O^+ fraction > 0.8. Notably, the ICON/IVM-Swarm pairs exhibit a stronger agreement than the ICON/IVM-JULIA pairs. Furthermore, Fig. 8a demonstrates that the RMSE can be reduced to less

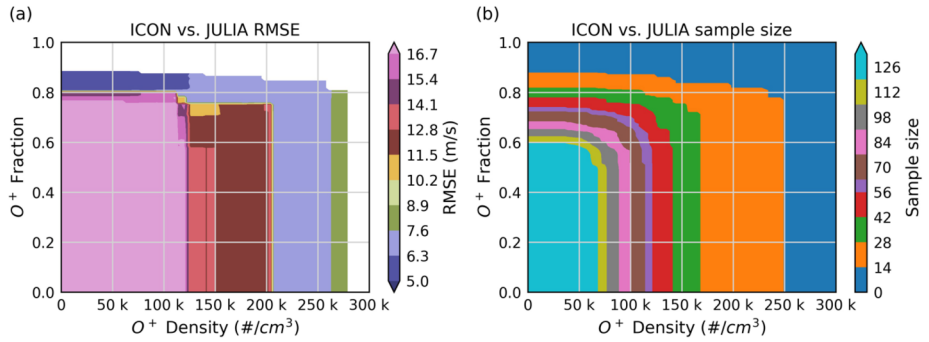

Fig. 6 (a) RMSE between vertical drift measurements from ICON/IVM and JULIA, considering the corresponding O^+ fraction and O^+ density as the lower limit for data selection from all conjunctions between 10 and 17 LT in 2020 and 2021 (Fig. 5c). (b) Similar plot as in (a), but displaying the sample size under the corresponding O^+ fraction and O^+ density limit

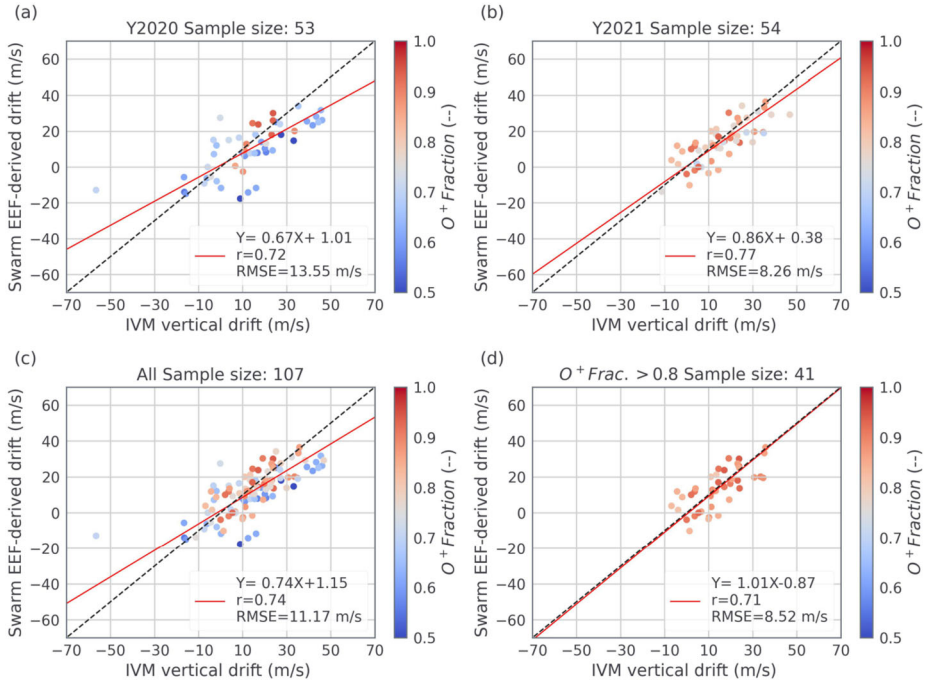

Fig. 7 Same as Fig. 5 but comparing ICON/IVM vertical drift with the drift derived from the equatorial zonal electric field of Swarm-A. Successful ICON/IVM-Swarm conjunction is when IVM is within 2000 km from Swarm-A, with measured time difference less than 20 minutes

than 10 m/s for ICON/IVM-Swarm pairs by requiring an O^+ fraction > 0.7 or O^+ density $< 5 \times 10^4/\text{cm}^3$ compared to the O^+ fraction > 0.8 or O^+ density $< 2 \times 10^5/\text{cm}^3$ criteria needed for ICON/IVM-JULIA pairs to achieve the same level of RMSE. Alongside the high correlation, the slope approaches unity for the ICON-Swarm pairs, and the overall RMSE when O^+ fraction > 0.8 is 8.52 m/s.

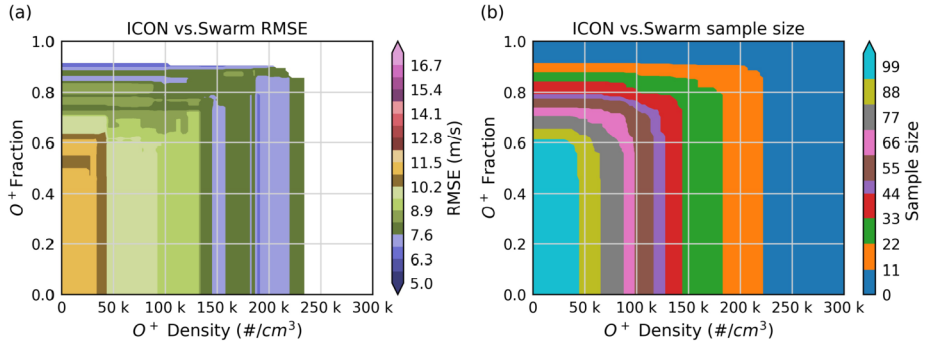

Fig. 8 (a) RMSE between vertical drift measurements from ICON/IVM and Swarm, considering the corresponding O^+ fraction and O^+ density as the lower limit for data selection from all conjunctions between 10 and 17 LT in 2020 and 2021 (Fig. 7c). (b) Similar plot as in (a), but displaying the sample size under the corresponding O^+ fraction and O^+ density limit

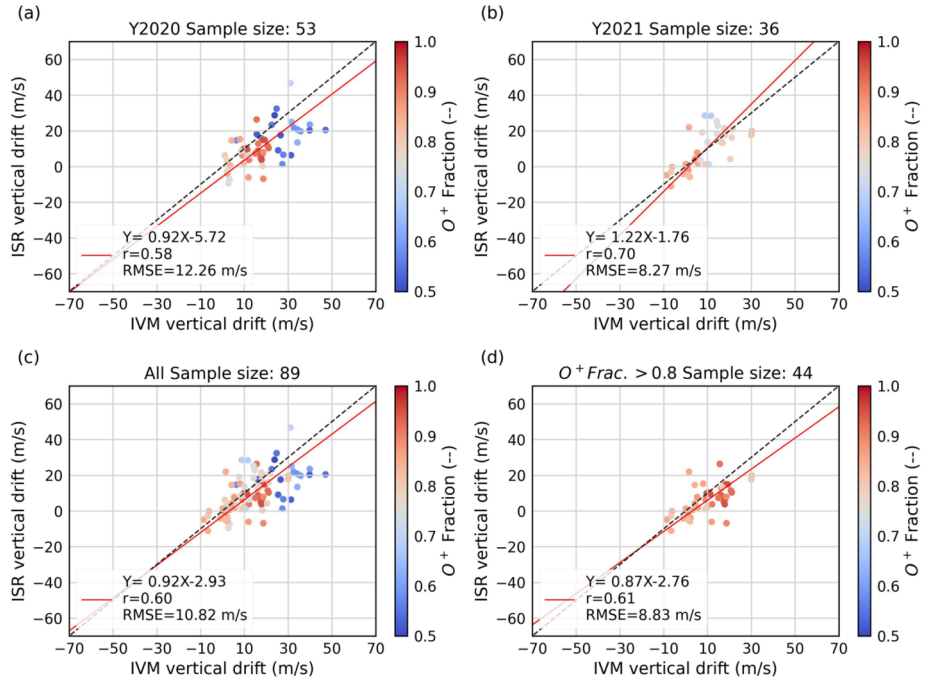

Fig. 9 Same as Fig. 5 but comparing ICON/IVM vertical drift with the vertical drift measured by ISR between 570 and 600 km altitude between 11 and 17 LT. Successful ICON/IVM-ISR conjunction is when IVM is within 20 degrees longitude and 5 degrees latitude from JRO, with measured time difference less than 20 minutes

ICON/IVM-ISR conjunctions provide the one-to-one comparison of vertical drift at ICON altitude (∼575 km). In Fig. 9, we compare the ISR vertical drift data which error less than 10 m/s averaging over 550 km to 600 km with in-situ ICON/IVM measurements. 2021 has better correlation and RMSE than 2020 just like the other comparisons. In general,

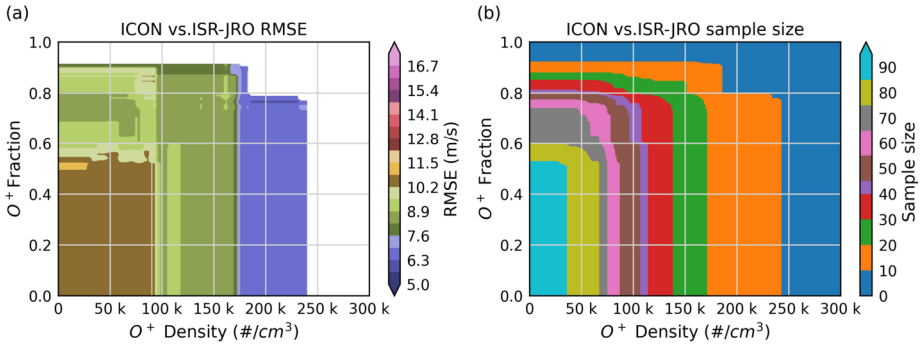

Fig. 10 (a) RMSE between vertical drift measurements from ICON/IVM and ISR, considering the corresponding O^+ fraction and O^+ density as the lower limit for data selection from all conjunctions between 10 and 17 LT in 2020 and 2021 (Fig. 7c). (b) Similar plot as in (a), but displaying the sample size under the corresponding O^+ fraction and O^+ density limit

the slope between ICON/IVM and ISR is close to 1 even before applying the restriction of O^+ Fraction. It implies again that the accuracy of ICON/IVM is trustworthy, as we stated in the comparison between ICON/IVM and Swarm. Also, Fig. 10 shows a less stringent requirement for achieving an RMSE of less than 10 m/s, which involves having an O^+ fraction > 0.55 and O^+ density of 1×10^5 /cm^3. Using the same criteria as we applied to the conjunctions with Swarm and JULIA, the resulting RMSE and r of ICON/IVM-ISR conjunctions under O^+ fraction >0.8 is 8.83 m/s and 0.61.

4 Revisiting the 24-hour Running Mean Removal Method in Immel et al. (2021)

The comparisons between ICON and the JULIA and Swarm instruments provide valuable insights into understanding the potential sources of variation in the ICON/IVM measurements, whether they stem from geophysical factors or instrumental efficiency. However, imposing the criteria of O^+ fraction > 0.8 for data selection would result in the exclusion of approximately 75% of the data collected in 2020. Alternatively, Immel et al. (2021) proposed a pre-processing step that involves removing the 24-hour mean from all the original meridional drift regardless of their latitudes. This approach is based on the expectation that the vertical drift exhibits an upward trend during the day and a downward trend during the night in low-latitude regions. Therefore, the 24-hour mean of the vertical drift is expected to be close to zero, which is consistent with the irrotational nature of the electric field. Nevertheless, it is important to acknowledge that this assumption may be violated if there are significant changes in the global electric field over a day, such as those induced by prompt penetration electric fields or planetary waves. The value of the 24-hour mean thus serves as an estimation of the systematic offset that necessitates correction to enhance the accuracy of the data.

Figure 11 provides a comprehensive view of the continuous IVM vertical drift data from January 2020 to the end of 2021. The top trace displays the 24-hour running mean, represented by the green solid line. It is evident that the 24-hour running mean of the vertical drift exhibits substantial fluctuations and deviates from zero before October 2020, while it becomes smoother and approaches zero thereafter. This pattern is also discussed by Heelis

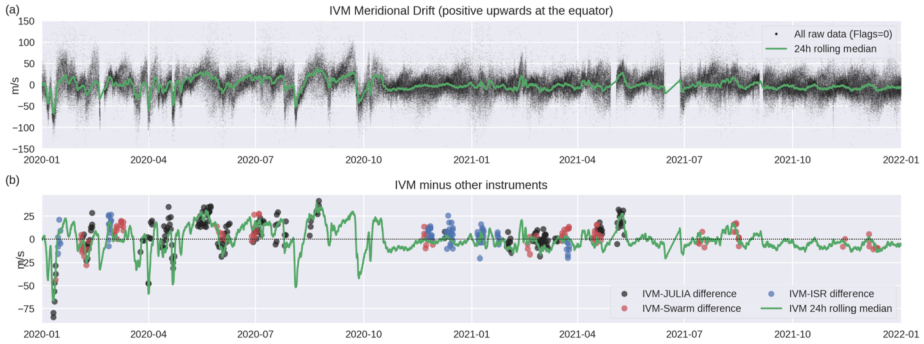

Fig. 11 (Top) IVM vertical drift measurements from December 6, 2019, to the end of January 2022. The green solid line represents the 24-hour running mean. (Bottom) Difference between various instruments and ICON/IVM overlaid on the 24-hour running mean vertical drift without the application of selection criteria

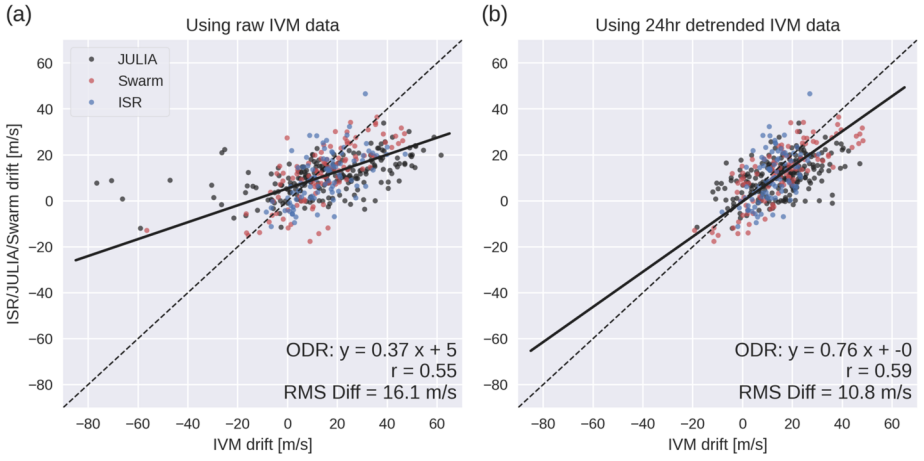

Fig. 12 Scatter plot comparing ICON/IVM drift measurements against drift measurements from other instruments selecting between 10 and 17 LT in 2020 and 2021. Panel (a) displays the scatter plot using raw IVM data, while panel (b) shows the scatter plot using 24-hour running mean detrended IVM data

et al. (2022), which indicate a noticeable correlation between the short-term excursions and the aperture potential, particularly when there is a significant population of H^+. These results further underscore the significance of the O^+ fraction as a key parameter for evaluating the data quality in 2020.

In the lower panel of Fig. 11, the conjunction measurements from JULIA, Swarm, and the ISR are superimposed on the 24-hour running mean without any filtering. Using JULIA, Swarm, and ISR as a reference, each dot in the lower panel represents a conjunction, indicating the difference between the IVM vertical drift and the vertical drift measured by the reference measurements. These comparisons manifest that the largest discrepancies between the IVM and the other instruments coincide with offsets in the IVM's 24-hour mean drift. Furthermore, Fig. 12 illustrates the comparison of drift data obtained from ICON/IVM before and after removing the 24-hour running mean. Figure 12a displays the raw data without any pre-processing, while Fig. 12b presents the same set of data after the 24-hour running

mean is subtracted. As shown in Fig. 12b, the pre-processing significantly reduces scattering and brings the slope closer to unity, changing from 0.37 in Fig. 12a to 0.76 in Fig. 12b. The RMSE is improved from 16.1 m/s before to 10.8 m/s after detrending the 24-hour running mean. The improvement of the correlation and RMSE in Fig. 12b highlights the effectiveness of removing the 24-hour running mean in mitigating errors while retaining data from the deep solar minimum with acceptable uncertainty.

One benefit of employing the 24-hour running mean removal method to mitigate uncertainty in ICON/IVM drift measurements is the utilization of nighttime data, where O^+ fractions tend to be below 0.8 regardless of the level of solar radiation. This approach allows for the inclusion and analysis of data collected during nighttime hours, which would otherwise be excluded based on the O^+ fraction criterion. Figure 13 showcases the agreement of vertical drift from ICON/IVM and ISR with respect to the LT frame. All ICON/IVM-ISR conjunctions recorded in 2020 and 2021 are included without any restrictions, but note that the first 3 panels from the top showing the correlation coefficient (r), RMSE, and slope are based on the data after 24-hour running mean removal. To ensure the statistical significance, LT bins shown in the plot are those sample size larger than 10. The data gap observed from 5 LT to 10 LT due to the implementation of quality control measures to account for the influence of photoemission within the instrument (Stoneback et al. 2012; Heelis et al. 2022). In summary, this analysis reveals a significant correlation ($r \sim 0.5$) between the vertical drift derived from ISR and IVM in the 13 to 16 LT range, with an RMSE of less than 13 m/s. This finding is consistent with the observations in Fig. 9 of Stoneback et al. (2011), which demonstrate a decent agreement between ISR and C/NOFS vertical drift during the same LT range. However, at 18 LT, the influence of the prereversal enhancement leads to an increase in RMSE. Overall, the RMSE during nighttime exceeds 20 m/s, significantly higher than the values observed in the afternoon sectors. This result is expected due to the presence of plasma bubbles and ionospheric scintillation during nighttime hours.

5 Discussion

Assessing the conjunctions without imposing O^+ fraction restrictions (Fig. 5c, Fig. 7c, and Fig. 9c), it is noticeable that the higher RMSE of ICON/IVM-JULIA conjunctions (22.96 m/s) compared to the conjunctions with both Swarm and ISR (around 11 m/s). Figure 11 and Fig. 12 provide clear evidence that the majority of IVM-JULIA conjunctions occurred before October 2020, during a period when IVM exhibited a significant displacement in its 24-hour running mean from zero. In contrast, the conjunctions with Swarm and ISR took place during a period when the displacement was less than 20 m/s. While Fig. 12 shows that 24-hour running mean removal method can effectively reduce the uncertainty in ICON/IVM drift, it is important to consider that the 24-hour running mean removal alone improves the RMSE to approximately 11 m/s, which is not better than the RMSE for the conjunctions with Swarm (Fig. 7c) and ISR (Fig. 9c) without the imposition of O^+ fraction restrictions. Therefore, achieving higher accuracy and precision still requires consideration of the ambient plasma environment. Additionally, it is worth acknowledging that this study may not have encompassed all factors contributing to the observed discrepancies. Further investigation is needed to explore potential influences such as spacecraft charging under low plasma density conditions.

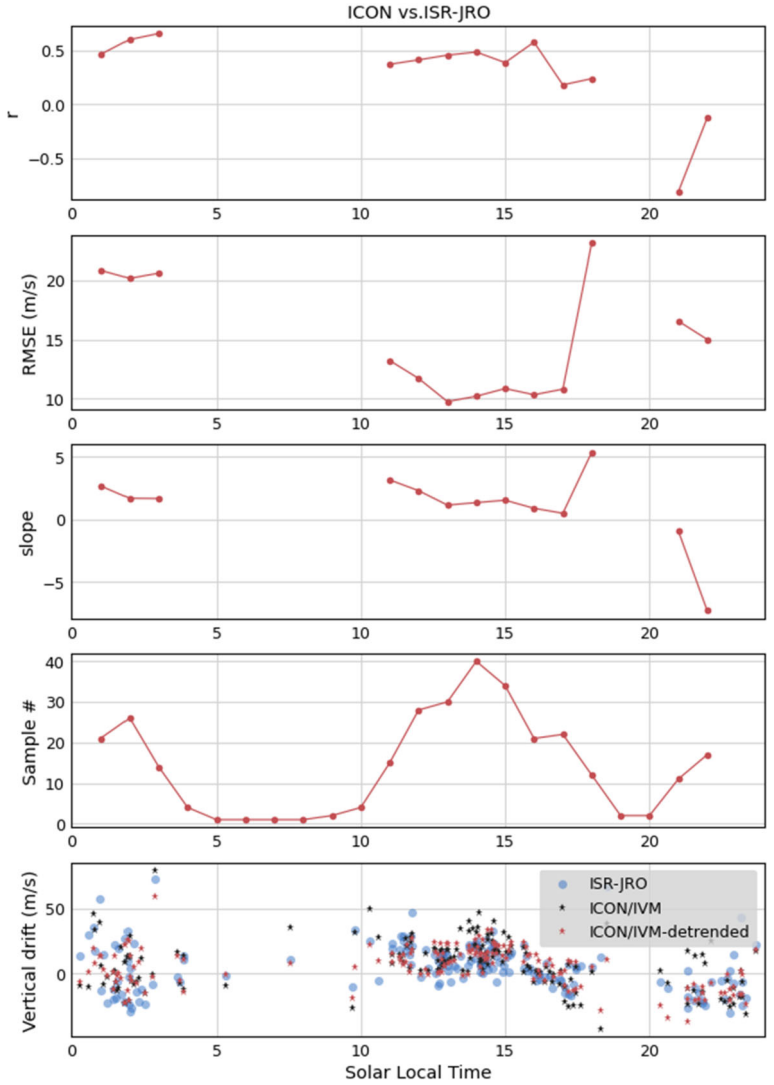

Fig. 13 Vertical drift comparison between ICON/IVM and ISR conjunctions as a function of solar LT without any constraint in O+ fraction. The panels display the correlation coefficient (r), RMSE, slope, and sample size. Each LT bin includes data from one hour before to one hour after the specified time. The vertical drift measurements from ISR, ICON/IVM, and ICON/IVM after detrending the 24-hour running mean are provided at the bottom panel

6 Conclusion

Upon revisiting the correlation analysis between Swarm/EEF data and the JULIA radar, a notable correlation coefficient of 0.89 is obtained. This outcome aligns with prior studies, affirming the persistence of the correlation even during the period of more solar minimum conditions in 2020-2021 when the ICON/IVM instrument was operational. To delve into the uncertainty of the vertical drift in ICON/IVM, comprehensive comparisons are made

with Swarm, JULIA mode, and ISR vertical drift measurements. Without imposing any restrictions, the ICON/IVM shows favorable agreement with Swarm and ISR, displaying an approximate RMSE of 11 m/s. However, in the case of the ICON/IVM-JULIA conjunctions, a larger RMSE of 22 m/s is observed, primarily attributed to numerous conjunctions occurring during instances of significant offset in the 24-hour mean drift. To ensure statistical significance and enhance the agreement with JULIA, a minimum O^+ fraction of 0.8 is employed, resulting in a reduced RMSE of 7.4 m/s between ICON/IVM and JULIA, and 8.5 m/s between ICON/IVM and Swarm. It is worth highlighting that the largest discrepancies between ICON/IVM and the other instruments arise when offsets in the 24-hour mean drift are present. By eliminating the 24-hour running mean from the ICON/IVM vertical drift data, these discrepancies are effectively mitigated, bringing the regression line closer to unity and maintaining data integrity from the deep solar minimum period with an acceptable level of uncertainty. By using the same methodology presented in this work, future missions could calibrate their drift measurement to facilitate meaningful integration with ICON measurement.

Acknowledgements The authors wish to express their gratitude to the engineering team and science data center of ICON. Special thanks to Rod Heelis for the valuable and insightful discussion. YJW wish to thank Claire Gasque and Colin Triplett for the valuable discussion to improve the quality of the paper. The work is supported by the Ionospheric CONnection Explorer (ICON) project contract number NNG12FA45C. BJH acknowledges funding by NSF AGS-2230365. The Jicamarca Radio Observatory is a facility of Instituto Geofísico del Perú operated with support of the NSF AGS-1732209 through Cornell University. AM is supported by ICON NASA grant 80NSSC21K1990. The ICON data is available at Space Physics Data Facility (SPDF) https://spdf.gsfc.nasa.gov/pub/data/icon/ and ICON science data center at UC Berkeley https://icon.ssl.berkeley.edu/Data. The authors would like to acknowledge the European Space Agency for making Swarm data available. The Swarm EEF data is available at https://swarm-diss.eo.esa.int/#swarm%2FLevel2daily%2FEntire_mission_data%2FEEF%2FTMS. F10.7 data is available at the OMNIWeb https://omniweb.gsfc.nasa.gov.

Declarations

Competing Interests No potential conflict of interest is identified. This research does not involve human participants and/or animals. All authors agreed with submitting the manuscript to Space Science Reviews.

References

Alken P, Maus S (2007) Spatio-temporal characterization of the equatorial electrojet from champ, Ørsted, and sac-c satellite magnetic measurements. J Geophys Res Space Phys 112. https://doi.org/10.1029/2007JA012524

Alken P, Maus S (2010) Relationship between the ionospheric eastward electric field and the equatorial electrojet. Geophys Res Lett 37:1–5. https://doi.org/10.1029/2009GL041989

Alken P, Maus S, Chulliat A, Vigneron P, Sirol O, Hulot G (2015) Swarm equatorial electric field chain: first results. Geophys Res Lett 42:673–680. https://doi.org/10.1002/2014GL062658

Chau JL, Kudeki E (2006) Statistics of 150-km echoes over Jicamarca based on low-power VHF observations. Ann Geophys 24(5):1305–1310 https://doi.org/10.5194/angeo-24-1305-2006

Chau JL, Woodman RF (2004) Daytime vertical and zonal velocities from 150-km echoes: their relevance to F-region dynamics. Geophys Res Lett 31:L17801. https://doi.org/10.1029/2004GL020800

Choi JM, Lin CCH, Panthalingal Krishanunni R et al (2023) Comparisons of in situ ionospheric density using ion velocity meters onboard FORMOSAT-7/COSMIC-2 and ICON missions. Earth Planets Space 75:15. https://doi.org/10.1186/s40623-022-01759-31

Chou MY, Braun JJ, Wu Q, Heelis RA, Zakharenkova I, Cherniak I et al (2021) Validation of formosat-7/cosmic2 ivm ion density and tgrs orbit electron density. Terr Atmos Ocean Sci 32. https://doi.org/10.3319/TAO.2021.06.22.01

Englert CR, Harlander JM, Brown CM, Marr KD, Miller IJ, Stump JE et al (2017) Michelson interferometer for global high-resolution thermospheric imaging (MIGHTI): instrument design and calibration. Space Sci Rev 212(1–2):553–584. https://doi.org/10.1007/s11214-017-0358-4

Freedman D, Pisani R, Purves R (2007) Statistics, 4th edn. WW Norton, New York, London

Friis-Christensen E, Lühr H, Hulot G (2006) Swarm: a constellation to study the Earth's magnetic field. Earth Planets Space 58:351–358. https://doi.org/10.1186/BF03351933

Harding BJ, Makela JJ, Englert CR, Marr KD, Harlander JM, England SL, Immel TJ (2017) The MIGHTI wind retrieval algorithm: description and verification. Space Sci Rev 212:585–600. https://doi.org/10.1007/s11214-017-0359-3

Harlander JM, Englert CR, Brown CM, Marr KD, Miller IJ, Zastera V et al (2017) Michelson interferometer for global high-resolution thermospheric imaging (MIGHTI): monolithic interferometer design and test. Space Sci Rev 212:601–613. https://doi.org/10.1007/s11214-017-0374-4

Heelis RA, Stoneback RA, Perdue MD, Depew MD, Morgan WA, Mankey MW et al (2017) Ion velocity measurements for the ionospheric connections explorer. Space Sci Rev 212(1–2):615–629. https://doi.org/10.1007/s11214-017-0383-3

Heelis RA, Depew MD, Chen YJ et al (2022) Ionospheric connections (ICON) ion velocity meter (IVM) observations of the equatorial ionosphere at solar minimum. Space Sci Rev 218:68. https://doi.org/10.1007/s11214-022-00936-w

Immel TJ, England SL, Mende SB, Heelis RA, Englert CR, Edelstein J et al (2018) The ionospheric connection explorer mission: mission goals and design. Space Sci Rev 214(1):13. https://doi.org/10.1007/s11214-017-0449-2

Immel TJ, Harding BJ, Heelis RA, Maute A, Forbes JM, England SL et al (2021) Regulation of ionospheric plasma velocities by thermospheric winds. Nat Geosci 14:893–898. https://doi.org/10.1038/s41561-021-00848-4

Kudeki E, Fawcett CD (1993) High resolution observations of 150 km echoes at Jicamarca. Geophys Res Lett 20:1987–1990. https://doi.org/10.1029/93GL01256

Kudeki E, Bhattacharyya S, Woodman RF (1999) A new approach in incoherent scatter F region E × B drift measurements at Jicamarca. J Geophys Res 104:28,145–28,162

Mende SB, Frey HU, Rider K, Chou C, Harris SE, Siegmund OHW et al (2017) The far ultra-violet imager on the icon mission. Space Sci Rev 212(1–2):655–696. https://doi.org/10.1007/s11214-017-0386-0

Rodrigues FS, Smith JM, Milla M, Stoneback RA (2015) Daytime ionospheric equatorial vertical drifts during the 2008-2009 extreme solar minimum. J Geophys Res Space Phys 120:1452–1459. https://doi.org/10.1002/2014JA020478

Schreiner WS, Weiss JP, Anthes RA, Braun J, Chu V, Fong J et al (2020) Cosmic-2 radio occultation constellation: First results. Geophys Res Lett 47. https://doi.org/10.1029/2019GL086841

Shidler SA, Rodrigues FS (2019) On the magnitude and variability of height gradients in the equatorial f region vertical plasma drifts. J Geophys Res Space Phys 124:4916–4925. https://doi.org/10.1029/2019JA026661

Stephan AW, Meier RR, England SL, Mende SB, Frey HU, Immel TJ (2018) Daytime O/N_2 retrieval algorithm for the Ionospheric Connection Explorer (ICON). Space Sci Rev 214:42. https://doi.org/10.1007/s11214-018-0477-6

Stevens MH, Englert CR, Harlander JM, England SL, Marr KD, Brown CM, Immel TJ (2018) Retrieval of lower themospheric temperatures from O2 a band emission: the MIGHTI experiment on ICON. Space Sci Rev 214(1):4. https://doi.org/10.1007/s11214-017-0434-9

Stoneback RA, Heelis RA, Burrell AG, Coley WR, Fejer BG, Pacheco E (2011) Observations of quiet time vertical ion drift in the equatorial ionosphere during the solar minimum period of 2009. J Geophys Res 116:A12327. https://doi.org/10.1029/2011JA016712

Stoneback RA, Davidson RL, Heelis RA (2012) Ion drift meter calibration and photoemission correction for the c/nofs satellite. J Geophys Res Space Phys 117. https://doi.org/10.1029/2012JA017636

Wong CS, Chan WS, Kam PL (2009) A student t-mixture autoregressive model with applications to heavy-tailed financial data. Biometrika 96(3):751–760. https://doi.org/10.1093/biomet/asp031